Impact Of Design Current Density On The Cost And Reliability Of Superconducting Magnet Systems For Early Commercial MHD Power Plants

Author(s): A. M. Hatch, P. G. Marston, R. J. Thome, A. M. Dawson, W. G. Langton, and W. R. Mann

Session Name: Liquid Metal MHD and Magnets

SEAM: 21 (1983)

SEAM EDX URL: https://edx.netl.doe.gov/dataset/seam-21

EDX Paper ID: 1023

IMPACT OF DESIGN CURRENT DENSITY ON THE COST AND RELIABILITY OF SUPERCONDUCTING MAGNET SYSTEMS FOR EARLY COMMERCIAL MHD POWER PLANTS[a]

A. M. Hatch, P.G. Marston, R.J. Thome, A.M. Dawson, W.G. Langton, W.R. Mann

Plasma Fusion Center
Massachusetts Institute of Technology
Cambridge, Massachusetts 02139

ABSTRACT

The impact of the design current density on the estimated cost of large superconducting MHD magnet systems was investigated with the aid of design scaling and cost estimating computer codes. Major emphasis was placed on systems of the size required for linear MHD generators in the channel power output range of 100 to 1100 MWe. Copper-stabilized NbTi windings with average current densities from 0.75×10^7 A/m^2 to 2.5×10^7 A/m^2 were considered. Results indicated that design current density has a significant effect on system cost, particularly for systems in the lower range of powers considered. For example, a reduction of roughly 35% in overall magnet system cost would be expected when design current density is increased from 1.0×10^7 A/m^2 to 2.0×10^7 A/m^2 in magnets at the small end of the size range. A reduction of roughly 30% would be expected for the same current density increase in magnets at the large end of the size range.

The impact of design current on certain aspects of magnet reliability was also explored. Higher current density implies a smaller winding cross section with less space available for copper stabilizer, supporting substructure and insulation. Therefore, problems of stabilization become more critical. Practical limits for stability criteria including heat flux and ratio of liquid helium to conductor volume were examined in relation to overall winding current density. Quench protection was also investigated, in particular the problem of dumping stored magnetic energy into external resistors fast enough to prevent overheating of regions of normal conductor. Results indicated that provisions to assure adequate stability and protection become more complicated for higher current densities and larger magnet sizes, and reliability is reduced.

In final designs for large MHD magnets, selection of average current density should be based on careful consideration of its effects both on magnet cost and on criteria affecting reliability. Results of the overall investigation are summarized in curves of various parameters vs winding average current density, including magnet weight, magnet system estimated cost, conductor stabilizer current density, conductor copper-to-superconductor ratio and maximum terminal voltage under emergency discharge conditions.

[a]Supported in part by the Office of Fossil Energy, MHD Division, U. S. Department of Energy.

INTRODUCTION

High reliability and long service life are prerequisites for superconducting magnets for commercial MHD power plants. These prerequisites dictate conservatism in magnet design, which can be achieved more easily if design current densities are kept low. Low capital cost is also an important consideration for commercial size MHD magnets, because the cost of the magnet system represents one of the largest component costs in the MHD topping cycle.

In developing designs for commercial MHD magnets, tradeoffs must be made between the cost advantages of higher design current densities and the resulting greater risks and/or special design provisions associated with the higher current densities.

The main purpose of the study reported here was to obtain quantitative information on the effect of design current density on magnet cost. It was intended that the results of the study would be useful in future design work on commercial-size MHD magnets, particularly with regard to the tradeoffs between the cost advantages of high current density and the adverse effects on other aspects of the design.

For the limited number of computer-generated designs covered in this paper, characteristics at the extremes of the parametric range, though believable, do not necessarily represent good design practice. The fact that certain computed characteristics tend to exceed practical limits emphasizes the importance of careful cost/risk assessment when final designs are developed.

APPROACH

In reviewing MHD magnet designs developed in the past, it is noted that winding (average) current densities become lower as magnet size is increased. This trend is shown in Table I, which lists representative MHD magnet designs, both commercial-size and test-facility size, with current densities ranging from 1.15×10^7 A/m^2 for the largest to 2.85×10^7 A/m^2 for the smallest. Based on these data, the range from 0.75×10^7 A/m^2 to 2.5×10^7 A/m^2 was selected as appropriate for this study.

A series of magnet reference designs of different bore sizes, representing magnets for power plants in the 100 to 1100 MWe range, and all embodying the same design concepts, were used as a basis for the study. For each magnet size, at least three current densities between 0.75×10^7 A/m^2 and 2.5×10^7 A/m^2 were considered. With the aid of computer programs and using scaling techniques, the characteristics and estimated costs of magnets of each bore size and current density were calculated. Curves were then plotted to show how cost, weight and other characteristics varied with design current density.

Particular attention was given to characteristics relating to reliability and safety. For typical winding designs, the impact of increased current density on stability criteria such as copper-to-superconductor ratio, heat flux and helium-to-conductor volume ratio were considered. Also considered were items such as the temperature rise in the winding when all stored magnetic energy is dumped into the winding as heat, and the peak terminal voltage when the magnetic energy is dumped into external resistors fast enough to prevent overheating of limited regions of normal conductor.

SIZES AND DESIGNS OF MAGNETS STUDIED

To cover the MHD channel power size range from 100 to 1100 MWe, three magnet bore sizes and active lengths were selected, based on the conceptual designs for the Engineering Test Facility (ETF)[1], the Commercial Demonstration Plant (CSM) [2] and a Large Baseload (LBL) system. The first two designs were developed in 1979-1981 as a

TABLE I

DESIGN CHARACTERISTICS

REPRESENTATIVE MHD MAGNET DESIGNS

Magnet Identification		U25	CDIF	CFFF	ETF	CASK	CSM
Field	T	5	6	6	6	6	6
Warm bore inlet aperture	m	0.4 dia.	0.78 x 0.97	0.8 dia.	1.5 x 1.9	2.48 dia.	2.2 x 2.8
Active length [a]	m	2.5	3.4	3.2	11.7	14.5	14.5
Stored energy	MJ	34	240	216	2900	6300	7200
Build	m	0.364	0.622	0.53	0.95	0.74	1.08
Design Current	kA	0.89	6.13	3.675	24.4	50.0	52.2
Current density, winding	10^7 A/m^2	2.82	1.87	2.0	1.42	1.28	1.15
Current density, conductor	10^7 A/m^2	5.0	6.28	2.63	8.16	2.2	5.7
Type of conductor	--	Rect. Built-up	Squ. Built-up	Rect. Built-up	Round Cable	Rect. Built-up	Round Cable
Substructure material	--	Fiber-glass & St. Steel [b]	Fiber-glass [b]	Fiber-glass [b]	Fiber-glass	St.Steel	Fiber-glass

Notes: a. Active length for all magnets is distance between on-axis field points of 0.8 B_{peak} at inlet and 0.6 B_{peak} at exit.

b. Banding between winding layers is used in place of a rigid substructure.

part of the DOE Magnet Technology Development Program. [3] The basic characteristics of the third design (LBL) were developed specifically for this study by scaling from the CSM design.

In addition to these three relatively large designs, a smaller magnet design, based on the Component Development and Integration Facility (CDIF) superconducting magnet [4] was also included in the study for comparative purposes. Basic characteristics of the four magnet designs considered are listed in Table II.

For consistency in the study itself, all designs used are of the rectangular saddle-coil type with rectangular warm bores, copper-stabilized NbTi conductor and rectangular frame winding support structures of stainless steel. Designs of other types, such as circular saddle coils with circular warm bores, would be expected to show the same trends with regard to the impact of current density on magnet cost and other characteristics.

For uniformity in comparing overall magnet characteristics, all magnet designs used in the study incorporated round cable conductors and insulating (fiberglass) substructures of the type used in the ETF magnet conceptual design [1] and shown in Fig. 1. For the purpose of determining copper and superconductor volumes, it was assumed that magnet windings were ungraded.

CALCULATION METHOD

A model to serve as a basis for the calculation of magnet characteristics was established as follows:

The winding configuration used was a rectangular saddle coil winding as shown in Fig. 2, generally similar in shape to the windings of the ETF, CSM and CDIF/SM designs[1,2,4]. A section through the winding, perpendicular to the axis and in the plane of peak-on-axis magnetic field (Plane P in Fig. 2) is shown in Fig. 3.

Design (winding) current density as referred to in this paper is the average current density in the winding cross section, shown in Fig. 3, required to produce the design field at the MHD channel axis.

To lower (or raise) the design current density while maintaining constant magnetic field on axis (at point 0), the area of the winding cross section is increased (or decreased) by varying the build, b, and width, d, as illustrated in Fig. 3.

For purposes of the study the following relationships were used:

$$I = 2aj \tag{1}$$

$$B = \frac{4It}{t^2 + s^2} \times 10^{-7} \tag{2}$$

where:

I = total ampere turns in winding (A)

a = area of winding cross section, one quadrant (m^2)

j = design current density (A/m^2)

B = peak on-axis field (T)

t = distance from Z axis to coil center, one quadrant (See Fig. 3)

s = distance from Y axis to coil center, one quadrant (See Fig. 3)

Combining (1) and (2)

$$j = \frac{B(t^2 + s^2)}{8at} \times 10^7 \qquad (3)$$

When varying b, it was assumed that good field uniformity in the channel cross section would be assured by restricting the center of coil quadrant cross section to lie on the radial line O-A. It was assumed also that the dimensions e and m would remain constant for a given magnet bore size to provide necessary space for structure and vacuum insulation.

Equation (2) calculates the field produced by infinitely long, parallel current filaments. It is therefore a means only of obtaining an approximation of the field at the axis of the saddle coil system, which is finite in length, tapered and has crossovers. However, experience has shown that results using Eq. (2) and an empirical correction factor are sufficiently accurate for the purposes of a study such as this.

An initial computer program, Scaler 1, was written to calculate the characteristics of a series of windings of different current densities for given bore sizes, active lengths and field strengths.

The input to Scaler 1 included data defining the basic geometry (size) of the magnet and specifying the general characteristics of the conductor, insulation and substructure. Winding current density was established by specifying the winding build (dimension b in Fig. 3).

The output included winding current density, ampere turns, insulation and substructure volume, superconductor volume, copper-to-superconductor ratio, winding overall dimensions and scaling factors.

A second computer program, Scaler 2, was written to calculate stored magnetic energy, component weights and budgetary costs using scaling techniques. The input included dimensions, volumes and scaling factors from the output of Scaler 1 together with baseline magnet characteristics (for scaling) and empirical cost data obtained from past experience in the costing of MHD magnets[1,6,7].

The output included stored energy, component weights and costs, and weights and costs for the assembled and installed magnet systems.

INPUT DATA

Specific data input to Scaler 1, used to arrive at the results reported in the following sections, are listed in Table III. For the 4, 100, and 450 MWe sizes, the data listed are consistent with the actual designs of the CDIF/SM, ETF and CSM magnets[4,2,1] respectively. For the 1100 MWe size, the data are extrapolations from CSM data.

The level of design currents used in the larger magnets is consistent with an earlier study[8] to investigate the impact of design current on magnet system cost. The study showed magnet system cost to be minimum for design currents in the range of 50

TABLE II

BASIC CHARACTERISTICS OF MAGNET REFERENCE DESIGNS USED IN STUDY

Magnet Identification	MHD Channel Power Output	Warm Bore Size Inlet	Warm Bore Size Exit	Active Length
	MWe	m	m	m
CDIF/SM	4	0.78 x 0.97	0.97 x 0.97	3.4
ETF	100	1.5 x 1.9	2.2 x 2.8	11.7
CSM	450	2.2 x 2.8	4.0 x 4.2	14.5
LBL	1100	3.3 x 4.2	6.1 x 6.4	16.0

Note: Field strengths for all magnets are taken as 6 T peak on-axis, 4.8 T inlet, 3.6 T exit.

TABLE III

SPECIFIC DATA INPUT TO SCALER 1

Magnet size (nominal MHD channel power)	MWe	4	100	450	1100
Reference		CDIF	ETF	CSM	LBL
Conductor type assumed	--	Cable	Cable	Cable	Cable
Conductor shape factor*	--	0.785	0.785	0.785	0.785
Conductor metal space factor**		0.547	0.547	0.547	0.547
Substructure design stress	10^8Pa	1.03	1.03	1.10	1.25
Design current	kA	6.13	25	50	80

* conductor shape factor = $\frac{\text{conductor envelope area}}{\text{area of square enclosing envelope}}$

** conductor metal space factor = $\frac{\text{conductor metal cross-sectional area}}{\text{conductor envelope cross-sectional area}}$

to 150 kA.

The substructure for all magnets was assumed to be a glass-reinforced plastic, designed to transmit magnetic loads from individual conductors to the surrounding coil containment vessels and superstructure without any accumulation of loading on the conductors themselves.

The superstructure for all four magnet sizes was assumed to be similar in design to that of the ETF magnet, made of stainless steel with design stress not exceeding 4×10^8 Pa.

Data input to Scaler 2 included the winding dimensions, volumes and scaling factors generated by Scaler 1 together with material densities, unit cost data and empirical cost factors derived from past experience. Typical data input to Scaler 2, common for all four sizes, are given in Table IV.

Unit cost of conductor was obtained from the curve of cost vs copper-to-superconductor ratio, Fig. 4. This curve was based on engineering estimates of unit costs of conductors of various copper-to-superconductor ratios, using the round cable conductor of the ETF magnet[1] as a model.

OUTPUT DATA

Partial Scaler 1 and Scaler 2 outputs are shown in Table V, which lists the computed major characteristics and costs for a particular magnet size (450 MWe) at two current density levels.

Computer output data were used to plot curves of magnet weight, cost and other characteristics vs design (winding) current density for four magnet designs with current densities varying from 0.75×10^7 A/m^2 to over 2.5×10^7 A/m^2. These data are discussed in the following sections.

WEIGHT AND COST

Curves of normalized magnet weight vs current density are shown in Fig. 5 for all four magnet sizes studied. Curves of normalized magnet cost vs current density are shown in Fig. 6. In both cases, normalizing is on the basis of the 1.0×10^7 A/m^2 designs.

It will be noted that the impact of design current density on magnet cost is significant. The curves indicate that increasing current density from 1.0×10^7 A/m^2 to 2.0×10^7 A/m^2 results in a decrease in magnet cost of about 30% in the case of the large baseload (1100 MWe) magnet and about 35% in the case of the (smaller) engineering test facility (100 MWe) size.

The decreases in total magnet weight and cost as current density increases are the result of accumulated decreases in weight and cost of all major components and associated decreases in winding and assembly costs. Higher current density implies a more compact winding which in turn means fewer ampere turns, decreased stored energy and total force, decreased volume of conductor and substructure and smaller helium containment vessel, superstructure and vacuum vessel. These trends for a particular magnet are shown in Table V, which lists calculated component weights for two current density levels in the CSM size (450 MWe) magnet.

STABILITY CRITERIA

Copper-to-superconductor ratio, heat flux and helium-to-conductor-metal volume ratio

TABLE IV

TYPICAL DATA INPUT TO SCALER 2

Density, stabilizer (copper)	8900	kg/m^3
Density, superconductor (NbTi)	6380	kg/m^3
Density, substructure (fiberglass)	1800	kg/m^3
Unit cost, substructure	10.35	\$/kg
Unit cost, helium vessel	18.00	\$/kg
Unit cost, superstructure	18.00	\$/kg
Unit cost, thermal shield , piping, etc.	58.00	\$/kg
Unit cost, vacuum vessel	14.00	\$/kg

TABLE V

MAJOR CHARACTERISTICS OF COMPUTER-GENERATED MAGNET DESIGN, 450 MWe SIZE, DESIGN CURRENT DENSITIES 1.2×10^7 A/m^2 AND 2.0×10^7 A/m^2

Peak on-axis field (input)	(T)	6	
Inlet aperture size (input)	(m)	2.2 x 2.8	
Active length (input)	(m)	14.5	
Design current (input)	(kA)	50	
Design current density	(10^7 A/m^2)	1.2	2.0
Ampere turns	(10^6 A)	38.6	34.8
Stored energy	(10^6 J)	7560	6100
Weight of conductor	(10^3 kg)	274	96
Weight of superstructure	(10^3 kg)	704	567
Total weight, magnet assembly	(10^3 kg)	2220	1580
Vacuum jacket overall length	(m)	21.7	21.1
Vacuum jacket overall diameter	(m)	12.8	11.5
Cost of magnet assembly installed, not including design costs, accessory costs, mark-up, etc.	10^6 \$	62.4	45.4
Total cost of magnet system including design, accessories, mark-up, etc.	10^6 \$	91.3	68.2

are criteria often used as measures of the stability, and hence the reliability of magnet windings. In the past, conservative winding designs for MHD magnets have usually involved copper-to-superconductor ratios in the range of 6 to 30, heat fluxes of less than 0.4 W/cm^2 and helium-to-conductor ratios of at least 0.2.

The effect of increasing design current density on stabilizer current density, copper-to-superconductor ratio and on heat flux, for the four magnet sizes studied, is shown in Figs. 7, 8 and 9.

It will be noted in Fig. 8 that copper-to-superconductor ratio decreases rapidly as winding current density is increased. The situation is compounded because the computer program keeps substructure stress constant, thus causing the absolute volume of substructure to drop only very slowly and the ratio of substructure to conductor to increase substantially as winding current density increases. This occurs because as the winding becomes more compact, there is less room for copper. Above 1.5×10^7 A/m^2 average current density, the copper-to-superconductor ratio in the larger magnets becomes lower and the current density in the stabilizer becomes higher than is usually considered acceptable. It should be kept in mind that the study is based on a specific type of conductor and winding design (round cable, uncompacted, with relatively low stressed substructure, see Fig. 1). By altering the conductor and winding designs and increasing substructure design stress, it is possible to increase the copper-to-superconductor ratio (with resulting decrease in stabilizer current density) but other factors such as cooling and substructure stress will be affected, and the designer must take these tradeoffs into account. The particular design selected for the study is not considered optimum, but is sufficiently representative to show trends.

The curves of Fig. 9 show heat flux at a very conservative level for the lower design current densities but rising rapidly, above a current density of 1.5×10^7 A/m^2. The heat fluxes shown were calculated assuming all strands in the cable conductor to be cooled on 100% of their surface. This is probably an optimistic assumption. Therefore, the heat flux curves should be considered primarily as indicators of trends.

Helium-to-conductor metal volume ratio does not vary with current density in the designs covered in this study, because all designs use a cable-type conductor with a metal-to-void ratio of about 0.55. The amount of helium in close contact with the conductor strands is therefore about 0.45 of the conductor (envelope) volume. Since this is well above the 0.2 value often considered satisfactory, the designs studied are conservative in this respect. However, one means of improving the undesirably low copper-to-superconductor ratio mentioned earlier is to substitute a compacted cable or monolithic conductor in place of the ordinary cable used. Such a substitution would involve reducing the helium-to-conductor metal volume ratio and would require careful consideration.

SAFETY AND PROTECTION

Important factors in the safety of a magnet system are the emergency discharge characteristics and the thermal inertia of the winding.

In the event of an MHD flow-train emergency or a fault in the magnet itself, it may be necessary that the MHD magnet be discharged very rapidly for safety reasons. Therefore, MHD magnet systems include external (dump) resistors and switches which, when activated, connect the magnet coils in series with external resistors designed for the emergency discharge function.

Under certain magnet fault conditions, emergency discharge may take place with only a very small (poorly cooled) section of magnet winding in the normal state. This normal section will heat up rapidly, and it is necessary that discharge to the external resistors be accomplished rapidly to prevent overheating of the conductor.

Rapid discharge involves high initial voltage at the coil terminals and voltage may become a critical factor in the coil design.

Curves of initial emergency discharge voltage vs design current density are shown in Fig. 10. The curves are based on the assumptions that all energy is dissipated in the external resistors and discharge is rapid enough to prevent the normal section of conductor (under adiabatic conditions) from exceeding 300 K temperature.

The voltages shown on Fig. 10 for the larger magnets at higher current densities appear excessive. For a given winding current density, the discharge voltage may be lowered by several design means, including adding of copper to the conductor, increasing the design current (reducing inductance) and dividing the winding into sections with separate power supplies. The designer must make tradeoffs between these design measures (and their possible adverse effects on the system) and the indicated cost savings associated with higher design current densities.

If a normal (resistive) region could be made to propagate very rapidly throughout the entire magnet winding, nearly all the magnetic energy would be absorbed as heat in the winding itself. To illustrate what would happen under this special condition, curves of final winding temperature vs design current density are shown in Fig. 11. For these curves, it is assumed that all the magnetic energy is dissipated uniformly throughout the winding as heat. The curves show that for all magnet designs studied except the largest, the windings are capable of absorbing, as heat, all of the stored magnetic energy without exceeding room temperature. The curves are conservative in that they assume adiabatic heating of copper, with no allowance for heat absorbed by helium, NbTi and substructure, or for conduction of heat into vessel walls and main structure.

WINDING SUBSTRUCTURE

The effect of winding substructure on the results discussed earlier deserves attention.

All magnet designs used in the study incorporated substructures providing individual support for the conductors and transmitting magnetic loads from conductors to containment vessels (superstructure) without accumulation of loading on conductors themselves. Substructure design stress ranged from 103 MPa for the smallest design to 125 MPa for the largest.

By eliminating substructures and adding relatively thin insulation to separate conductors from each other electrically, a substantial amount of extra space would be made available for additional copper in the conductor. In a final magnet design, the advantages of the structural support provided by the substructure must be weighed against the advantages of higher copper-to-superconductor ratio which can be achieved if substructure is eliminated.

CONCLUSIONS

1. Increasing design current density causes a significant decrease in the cost of superconducting MHD magnets, although the effect is not as great in larger magnets as in smaller ones. For a specific design studied, the estimated cost of a 1100 MWe size MHD magnet system was reduced by about 30% (roughly \$20 x 10^6) when design current density was increased from 1.0 x 10^7 A/m^2 to 2.0 x 10^7 A/m^2.

2. Increasing design current density from 1.0 x 10^7 A/m^2 to 2.0 x 10^7 A/m^2 has a significant adverse effect on the ability to achieve winding stability and safety. This effect is particularly pronounced in the larger size

magnet designs.

3. In anticipation of future large MHD magnet construction, it is important that analysis, development testing and design studies be performed to enable the use of higher winding current densities with acceptable stability and safety, so that magnet designs will be more cost effective.

REFERENCES

1. Conceptual Design Engineering Report - MHD Engineering Test Facility 200 MWe Power Plant, prepared for NASA/LeRC for DOE by Gilbert/Commonwealth DOE/NASA/0224-1, Vol. 1-V, September 1981.

2. MHD Magnet Technology Development Program Summary, prepared for DOE by Plasma Fusion Center, MIT, 1982 (to be issued).

3. A.M. DAWSON, P.G. MARSTON, R.J. THOME, Y. IWASA, and J.M. TARRH, "The United States Superconducting Magnet Technology Development Program," *IEEE Trans. Mag.*, MAG-17(5): 1966-1969, 1981. (MT7-Karlsruhe).

4. A.M. DAWSON, ed., Proc. 1980 Superconducting Magnet Design Conference, MIT, Cambridge, MA, March 1980.

5. General Dynamics Convair Division Report No. CASK-GDC-031, Cask Commercial Demo Plant MHD Superconducting Magnet Systems: Conceptual Design Final Report, MIT PO ML-67466, December 1979.

6. General Dynamics Convair Division Report No. PIN78-182 Cask Commercial Demo Plant MHD Magnet: Budgetary (Cost Estimate) and Planning, Final Report, MIT PO ML-68221, February 1980.

7. A.M. HATCH, "MHD Magnet Cost Analysis and Estimation" (Course Notes), MHD Magnet Design Course, MIT, Cambridge, MA, July 1980.

8. R.J. THOME, R.D. PILLSBURY, JR., H.R. SEGAL, and B.O. PEDERSEN, "Impact of High Current Operation on the Cost of Superconducting Magnet Systems for Large-Scale MHD Operation," *Adv. Cryogenic Eng.*, 25: 12-18, 1981.

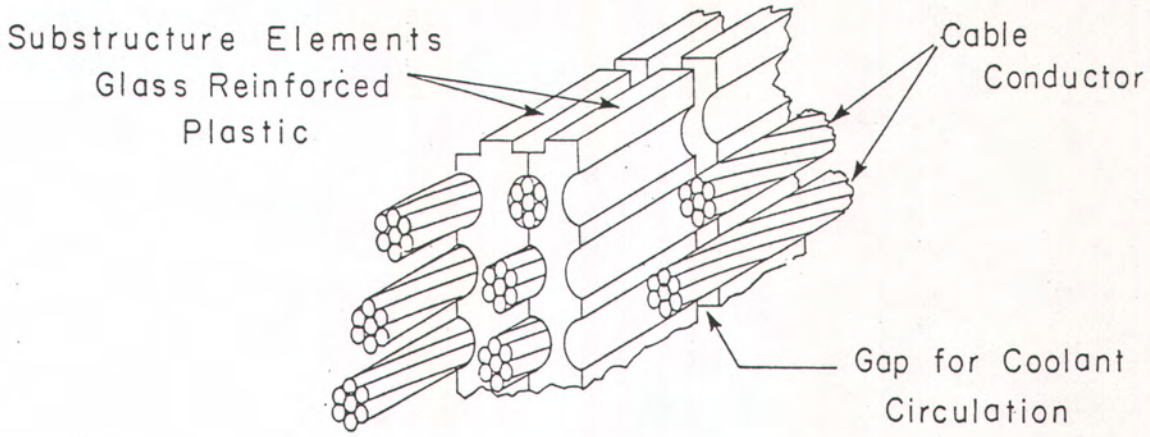

Figure 1 Magnet winding detail--round cable conductor supported in insulating substructure

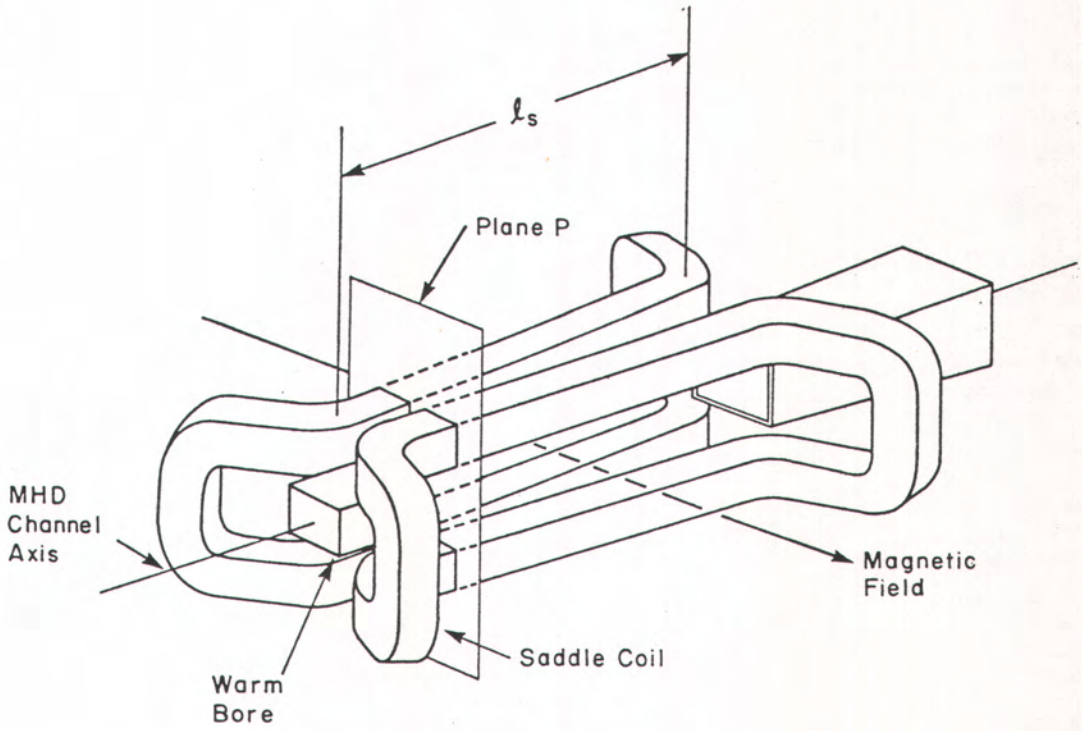

Figure 2 Rectangular saddle coil configuration

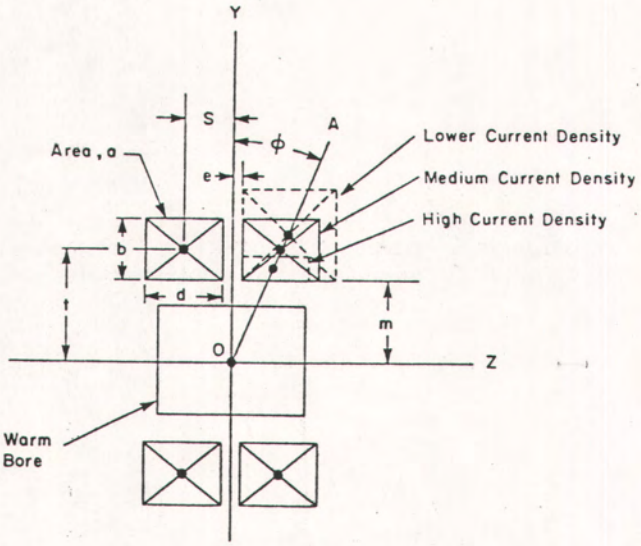

Figure 3 Winding cross section in plane of peak on-axis field

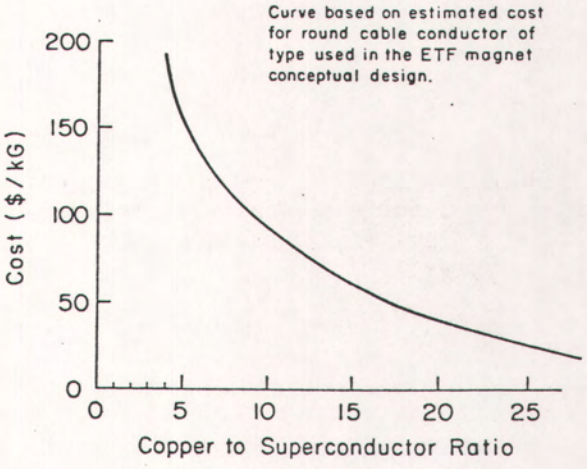

Figure 4 Curve of conductor unit cost vs copper-to-superconductor ratio

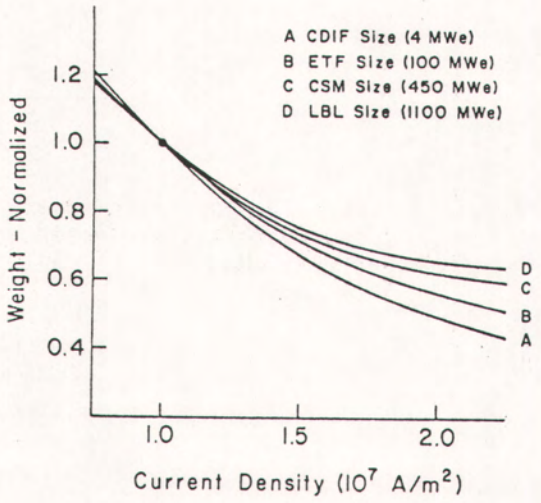

Figure 5 Curves of normalized magnet weight vs design current density

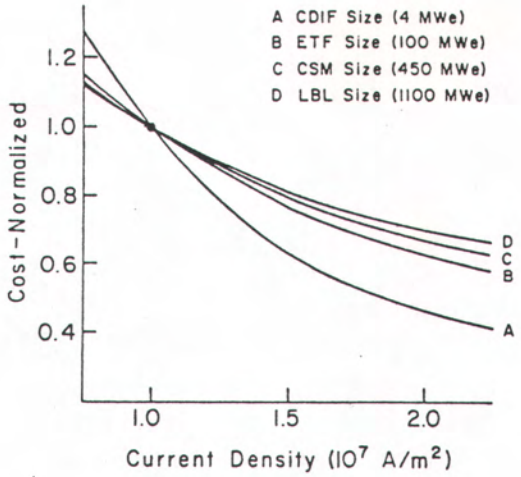

Figure 6 Curves of normalized magnet cost vs design current density

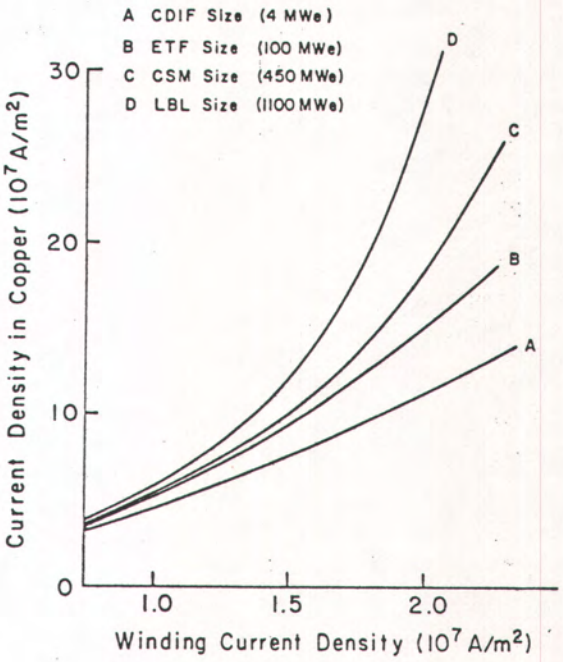

Figure 7 Curves of stabilizer (copper) current density vs design winding current density

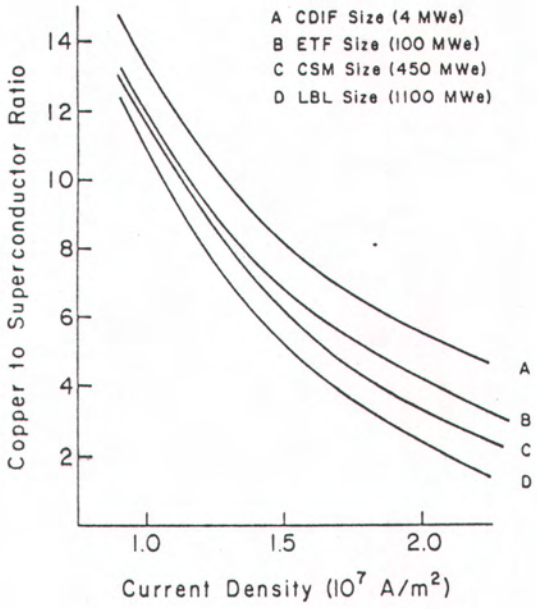

Figure 8 Curves of copper-to-superconductor ratio vs design current density

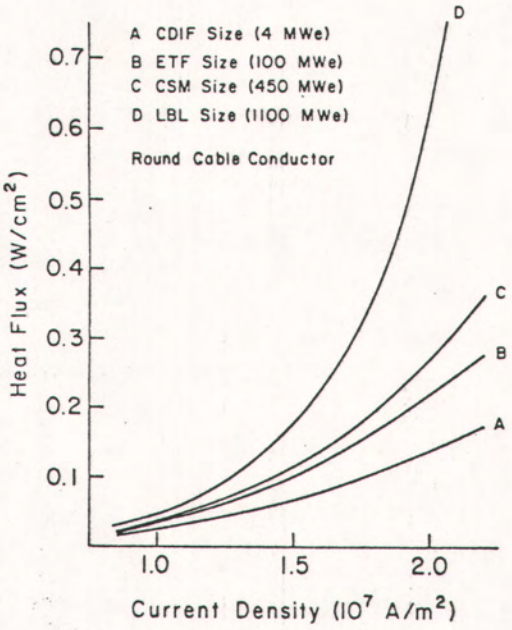

Figure 9 Curves of heat flux vs design current density

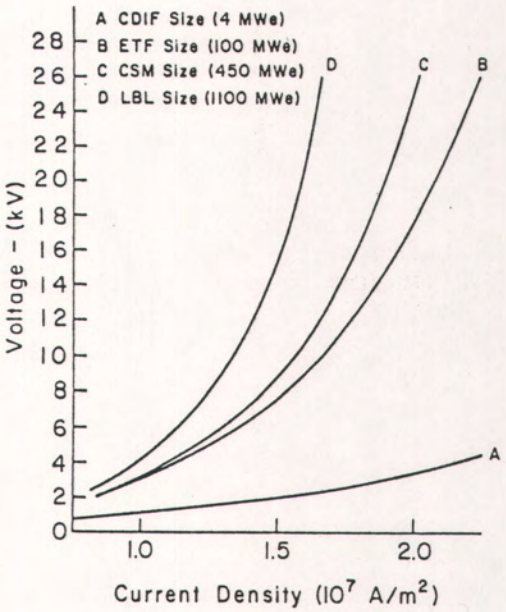

Figure 10 Curves of emergency discharge voltage (initial) vs design current density

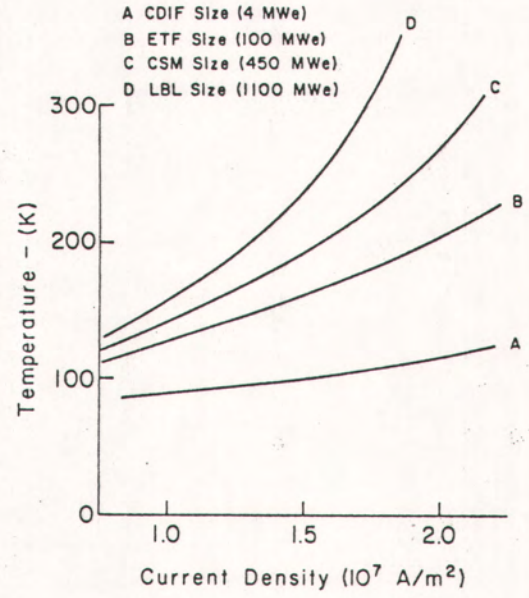

Figure 11 Curves of final conductor temperature vs design current density